



**FLUCOME 2009**

**10th International Conference on Fluid Control, Measurements, and Visualization  
August 17–21, 2009, Moscow, Russia**

## **APPARATUS FOR LASER GAS DIAGNOSTICS WITH THE USE OF FOCUSED BEAMS**

Sergey Fedorov<sup>1</sup> and Boris Boyarshinov<sup>2</sup>

### **ABSTRACT**

The new equipment for gas phase diagnostics was developed. It allows application of different nonintrusive optical methods: Rayleigh and Raman scattering, CARS (coherent antistokes Raman scattering), DB CARS (dual broadband CARS), and LIF (laser-induced fluorescence). This provides a possibility to obtain data on several physical parameters: local density, temperature, concentration of main components and radicals. This device includes the laser system, registration system with an optical multichannel analyzer, PC for data storage and processing, and software package for analysis of spectral data. It was applied to study pulse and turbulent reacting flows with high spatial ( $\sim 0.1 \text{ mm}^3$ ) and temporal ( $\sim 10^{-8} \text{ s}$ ) resolutions. This technique is transportable; it is mounted on the bearing structure, which can be adapted for experiments on various known aerodynamic installations. At the Institute of Thermophysics, we have used the laser methods for diagnostics of different flows: from the flows of rarefied and diluted gases to the flows of combustion products under the increased (up to 4 MPa) pressures and temperatures (about 3100 K).

**Keywords: Laser, scattering, fluorescence, combustion, radical.**

### **INTRODUCTION**

The modern experimental studies on the processes in gas flows set strict requirements to the applied tools of diagnostics. Only the non-contact measurements with high temporal and spatial resolution are applicable for the studies of chemically aggressive media at increased temperatures, pressures and velocities, typical for simulation of a space flight. For instance, the hypersonic wind tunnels support the stationary test conditions during  $\sim 0.05 \text{ s}$ . During this short period of time it is necessary to perform the non-contact measurements at gas flow velocity of up to 2 km/s, temperature of 200-3000 K and pressure of 0.01-100 atm. Spatial resolution should be  $\sim 1 \text{ mm}^3$ , temporal resolution should be  $\sim 10^{-5} \text{ s}$ ; and information about several physical parameters should be obtained during one run of a setup.

At the Institute of Thermophysics SB RAS the laser methods were used for diagnostics of different flows (from the flows of rarified gases to the flows of combustion products) under the increased pressures

---

<sup>1</sup> Corresponding author: Kutateladze Institute of Thermophysics, Siberian Branch, Russian Academy of Sciences, e-mail: [fedorov@itp.nsc.ru](mailto:fedorov@itp.nsc.ru)

<sup>2</sup> Kutateladze Institute of Thermophysics, Siberian Branch, Russian Academy of Sciences SB RAS

and temperatures. The equipment for pulse measurements of local gas parameters within the focused laser beams was developed. Its multiple functions are characterized by possibility to apply different optic methods: Rayleigh and Raman scattering (RS), coherent anti-Stokes Raman scattering (CARS), dual-broadband rotational CARS (DBCARS), and laser induced fluorescence (LIF). This equipment should be applicable for the studies at different gas-dynamic setups, including the installations of short-term action. To adapt it to the aerophysical experiments, the demands for the size construction characteristics at location near a test object were taken into account. To increase the measurement accuracy, the energy characteristics were approached to the limit ones. The goal of the current study is to provide brief information about abilities of this equipment and show the examples of its application.

## HARDWARE CONFIGURATION

A spectrometer consists of the laser and registration systems, mounted on the beam tables of the bearing construction. The laser system includes pumping laser, tunable laser on solutions of organic dyes and the scheme of laser radiation focusing (Fig.1.).

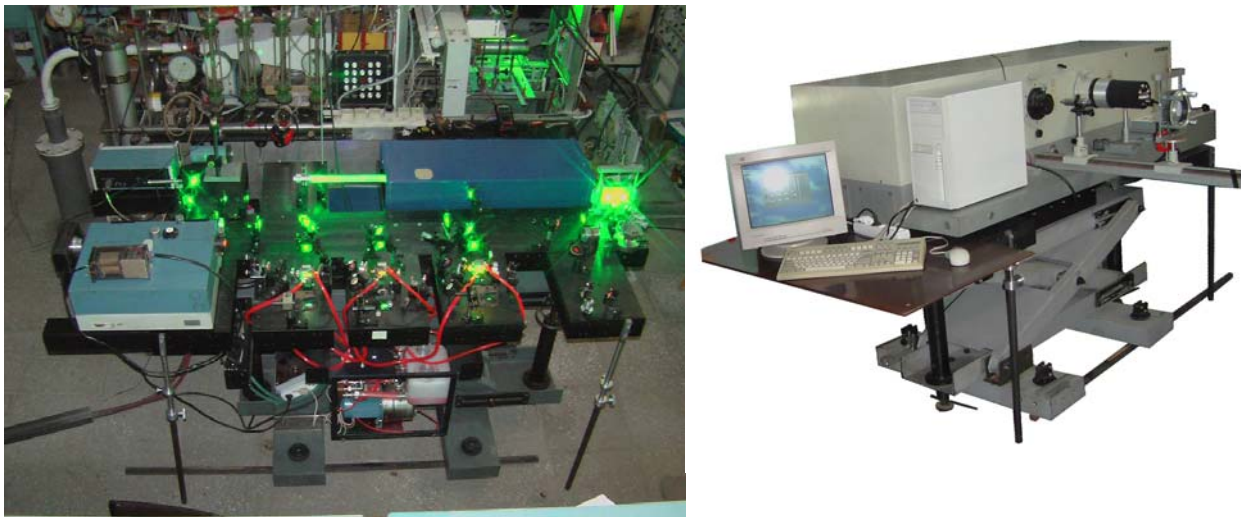


Fig. 1. In the left – laser system on the beam table. The wind tunnel for investigation of flow with combustion is in the background. In the right – registration system behind the wind tunnel.

### The bearing structure

The bearing structure is used for positioning of CARS-spectrometer units, for coordination of mutual position of laser beams, measurement object and registration system. It includes two similar beam tables. The table can be moved controllably in longitudinal and transverse directions and it can be rotated around the vertical axis. The upper part of this table is a flat surface of 300×2000 mm. The surface area of the table can be increased both longwise and widthway by means of additional platforms of 300×400 mm. The surface position above the floor level can be varied by a lifting mechanism at any height from 1000 to 1400 mm in accordance with the measurement point in the known aerodynamic devices.

### The pumping laser

The pumping laser is constructed by the scheme of pulse-periodic Nd:YAG-crystal laser with Q-switching. This laser consists of the master oscillator, emitting on one longitudinal and one transverse

modes; optic amplifier and frequency converter. The optic scheme of laser provides the mode of single-frequency generation and its long-term stability with relatively simple and compact construction. An emitter of solid-state laser is a unit of 920×340×200 mm. Radiation parameters are as follows: wavelength is 532 nm, energy is 0.5 J/pulse, pulse duration is 20 ns, beam divergence is  $\sim 10^{-3}$  rad., and repetition frequency is 5 Hz.

### The tunable laser

The tunable laser also consists of the master oscillator and several amplifying cascades with possibility of frequency transformation. The scheme of master oscillator is chosen depending on the problem. For instance, to achieve broadband radiation, a usual flat or weakly dispersive resonator is used. To achieve narrow-band radiation, a free flowing jet of a dye solution in ethylene glycol is used in the master oscillator. This oscillator consists of a flat dichroic mirror for pumping, grating (2400 grooves/mm) and a nontransmitting mirror. A beam, reflected specularly from the grating, acts as output radiation. The condition of single-mode generation is achieved by focusing of pumping radiation (into the size of 100  $\mu\text{m}$ ) through a quartz beam guide. To obtain a narrow generation line ( $\sim 0.001$  nm), the grating is put under the mode of grazing incidence. Gradual variation of radiation frequency within the required range is made by a change in mirror inclination by a microscrew with an electric drive. Each amplifying cascade is mounted on a separate platform. The delay lines of pumping radiation, required for coordination of generation times of pumping radiation, master oscillator and amplifiers, are located on some part of the beam table between the solid-state laser and amplifiers.

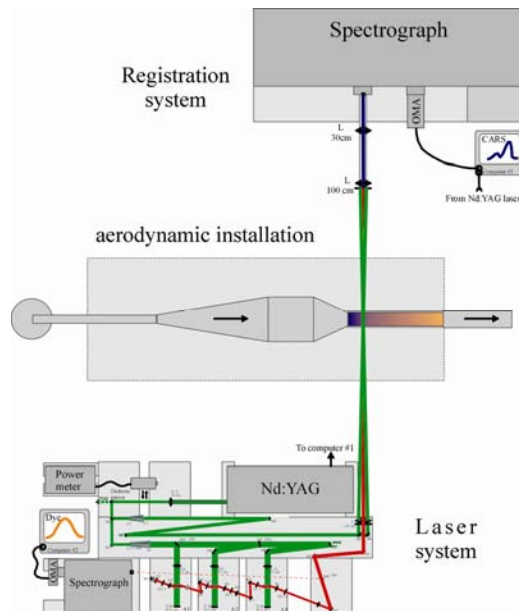


Fig.2. The scheme of CARS-spectrometer location at the wind tunnel.

### The scheme of radiation focusing

According to the multipurpose function of a device, three versions of the optic scheme are provided for the laser system, which allow application of the required diagnostic methods. They differ mainly by the schemes of master oscillator of the tunable laser and distribution of pumping radiation between amplifying cascades. The most complex (basic) version of the optic scheme is the scanning CARS. Other versions can be easily implemented changing the delays of pumping radiation and simplifying the scheme.

For the narrow-band CARS, two beams of narrow-band radiation are formed at the outlet of laser system: the reference (532 nm) and tunable (555-630 nm) ones. For the broadband CARS or DB CARS, there are also two beams: narrow-band reference and broadband tunable (with a band width of 4 or 15 nm) ones. For the LIF method, where radiation of the pumping laser is used completely, one beam is applied: a narrow-band tunable beam with frequency doubling (278-315 nm). For Raman or Rayleigh scattering only one beam of Nd:YAG laser is used.

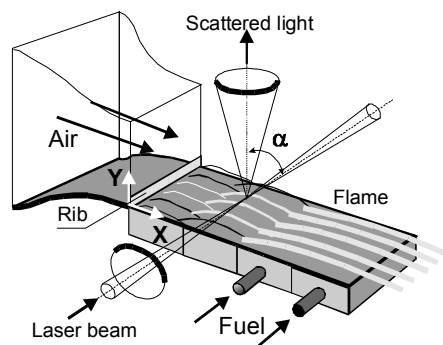


Fig.3. Orientation of laser beam and direction of scattered light gathering for measurements by the Rayleigh scattering, RS and LIF methods at a device with ethanol evaporation and combustion in a boundary layer.

The scheme of radiation focusing provides focusing and crossing for the laser beams at a measurement point, satisfying the requirements of phase-matching and adjustment of their polarization. If it is possible to locate the CARS-spectrometer near the measurement area, the focusing scheme is mounted on the front part of the beam table. For another case, the beam table with lasers will be moved to a suitable place, and the focusing scheme will be stayed on the periscope support near the test object.

### Registration system and data processing

The registration system allows distinguishing a light signal, its passing through a spectral device with limit resolution of  $\sim 1 \text{ cm}^{-1}$  and registration by a photodetector. A multichannel optic spectral recorder (CCD-sensor of  $0.2 \times 25 \text{ mm}$ , 2048 elements) with light amplifier or photomultiplier was used as a photodetector. It has a control volume, filled with gas, for control signal obtaining. It also includes a PC for data storage and processing, and software package for CARS-spectrometer control and calculation (analysis) of RS, CARS, DBCARS and LIF spectra of gases. The following parameters are used as the initial data for calculation: molecular constants, frequency and shape of the spectrum of laser radiation, resolution of a spectral device, state parameters of the studied gas (temperature, concentration, pressure, etc.). For the methods, based on the Raman effect, the following values are calculated: terms, level population, Raman frequency shifts, Placzek-Teller coefficients, Raman cross-sections and spectral line positions, linewidths, and, finally, frequency dependence of spectral intensity. For the LIF method the following values are calculated: terms, level population, line frequencies, Honl-London factors, cross-sections, linewidths, and frequency dependence of spectral intensity. The calculation algorithms are developed with consideration of selection rules for transitions between the levels, type of experimental scattering scheme, and convolution mechanisms. Calculation data can be shown in different windows: tables of parameters, population diagrams, and spectra. The software also allows the comparison of calculation spectra with the experimental one and optimization by the temperature and compositions. The software is written using the Visual C++ as a multidocument interface.

## APPLICATIONS

### Investigation of a vortex flow in the Ranque-Hilsch tube

This tube is widely used in different refrigerating and conditioning systems as a device for temperature separation of gas (Kuznetsov, 1994). There compressed air, rotating intensively in a limited volume, has a lower temperature near the axis and at the periphery its temperature is higher than at the tube inlet. At the tube outlet temperature difference between the “hot” and “cold” flows is about 20÷40K. The use of DB CARS method allowed us to obtain the rotational air spectra. By means of these spectra the temperature and mixture composition were determined. Then, the pressure at the measurement point was calculated (Boyarshinov & Fedorov, 1999).

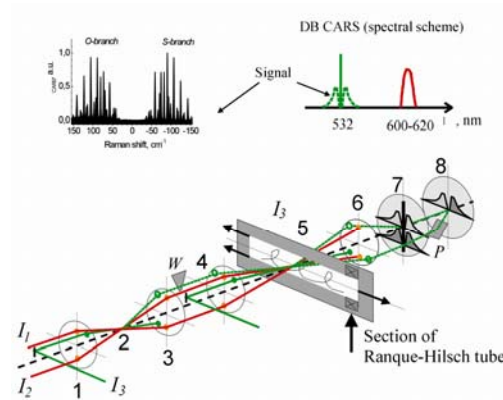


Fig.4. The scheme of experimental setup. Rotational air spectrum – superposition of nitrogen and oxygen spectra. The spectrum is overlapped in the vicinity of zero.

Laser beams (Fig.4) were focused twice and brought together by lenses (1 and 4) ( $f=180$  mm). The reference (2) and measurement (5) volumes with the sizes of  $0.1 \times 0.1 \times 2$  mm<sup>3</sup> were formed at the points of beam crossing. The choice of polarizations and beam positions on the focusing lenses provided their interaction at  $xyyx$ - and  $xyxy$ -components of nonlinear cubic susceptibility. The beams of scattered light from the reference and measurement volumes were sent to inlet slit (7) of the spectrograph, mutually separated in vertical direction because of the optical wedge (W). Laser illumination was suppressed by means of a shield. The S-branch of the spectrum from the measurement volume was superposed with the O-branch from the measurement volume in the outlet focal plane by inclination of a plane-parallel plate (P), mounted instead of a middle slit.

As it is shown in (Fedorov, 1996), in this combined spectrum (Fig.4) the symmetrical lines are generated by common spectral components of laser radiation. When processing spectral information, this allows the use of the branch from the reference volume for normalization, to reduce random measurement error.

The inner diameter of channel is 20 mm and the length is 350 mm. The air flow rate at the inlet to the four-slot (30 mm<sup>2</sup>) swirling device is 16 g/s, the flow rate through a diaphragm of 10-mm diameter at the “cold” outlet is 6.5 g/s. A change in coordinate Y by the value, multiple of 50 mm, was achieved by replacement of insertions, composing the channel. Data on the profiles of temperature, concentration and pressure were obtained for five cross-sections of the Rank-Hilsch tube with a step of 50 mm. According to profiles  $\overline{C}(N_2)$ , there was no air component separation in the studied flow with the accuracy of

measurement error.

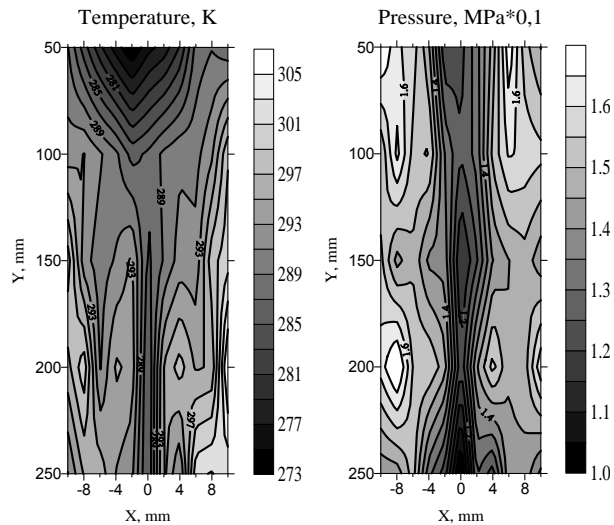


Fig.5.  $\bar{T}$  and  $\bar{P}$  distributions over the diametrical cross-section of the Rank-Hilsch tube.

The fields of ensemble mean  $\bar{T}$  and  $\bar{P}$ , plotted by their profiles, are shown in Fig. 5. It is clear that the temperature and pressure rise from the axis to the periphery. Longitudinal distribution of these parameters is nonuniform. In adjacent cross-sections there are the areas at one distance from the axis with pressure difference of up to 0.05 MPa. Considerable reduction of temperature occurs near the swirling device, where the outlet of “cold” air is located. According to quantitative data, there is a complex flow in the Ranque-Hilsch tube; these data demonstrate also the possibilities of the method for simultaneous measurements of three parameters of a gas mixture with a high spatial resolution.

### Temperature measurements of the products of solid fuel combustion under the high pressure

The pulse measurements of temperature were carried out in flame of the model fuel sample: stoichiometric mixture of ammonium dinitramide with polycaprolactone (Boyarshinov & Fedorov, 2002). This technique was based on the temperature dependence of the Q-branch shape in the CARS spectrum of nitrogen, contained in combustion products. The measurements were carried out under the pressure of 4 MPa at significant overlapping of spectral lines. The lasers with low radiation energy were used in these experiments; therefore, the simplified two-line CARS method was applied. Intensities of CARS signal, used for determination of combustion temperature, were registered at two frequencies. Calculated dependence between CARS signal intensity at these frequencies and temperature was used for data processing. Dependence of ensemble mean temperatures on time of sample combustion (0.5 s) was obtained. The temperature, averaged by instantaneous values, obtained in the range of 0.2-0.3 s, was 3097 K ( $\pm 3\%$ ). This value of rotational temperature of nitrogen in a jet of reaction products corresponds to a distance between the flame front and a measurement volume of about 5 mm. Therefore, the developed technique of local optic temperature measurements is applicable for investigation of combustion of substances, whose combustion products contain nitrogen.

## Measurement of temperature at hydrogen combustion

In experiments with hydrogen combustion in air at a flat burner with the length of 20 mm the instantaneous temperature was measured using the Q-branch of nitrogen. This flame extends the size of the area with a high temperature without pulsations, and it is a convenient object for equipment testing. The broadband CARS method with folded boxcars scheme, providing spatial resolution of several millimeters in longitudinal direction, was used.

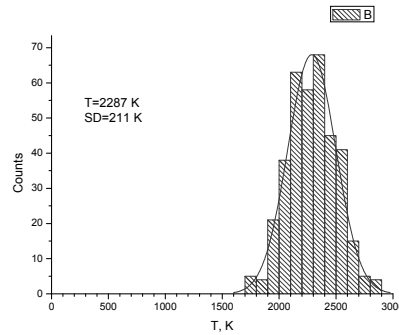


Fig.6. PDF at x=60 mm along the axis.

These temperatures correspond to the known data for hydrogen flame. The parameters, characterizing the accuracy of developed equipment with the initial radiation energy of 300 mJ/pulse, were obtained. It is shown that at the measurement of high temperatures of about 2300 K dispersion of instantaneous values is 211 K.

## Temperature measurements in a boundary layer with ethanol combustion

Before the development of CARS equipment, the pulse measurements of temperature were carried out with application of Rayleigh scattering method. Under some conditions, when turbulence of an incident flow was 8%, there was significant divergence (up to ~500 K) of the averaged temperatures, obtained by the probe and optic measurements. The reasons for this divergence can be, firstly, disadvantages of Rayleigh scattering method, subjected to the effect of parasite flare lights; secondly, there could be temperature alternation at the periphery of reacting boundary layer. It was assumed that the real reasons would be determined by direct measurements of instantaneous temperature by the CARS method.

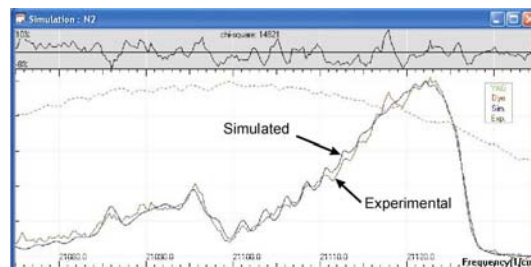


Fig.7. The software window, where the flame CARS spectrum and corresponding calculated spectrum are compared, and thus, this determines the temperature at the measurement point.

The method of broadband CARS with a planar scheme of laser beam convergence and spatial resolution in longitudinal direction of about 1 mm was used. Flame temperatures determined at turbulence of 8%, incident flow velocity of 10 m/s and flame stabilizer height of 3 mm are shown in the Fig.8.

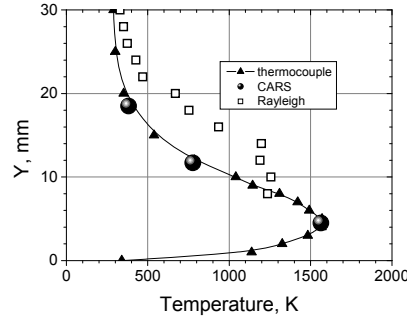


Fig.8. Comparison of the averaged temperatures, measured by different methods.

It is obvious that there is no divergence between the results of direct temperature measurements, performed by the CARS-spectrometer (circles) and a thermocouple (triangles). Squares indicate the results of indirect temperature measurements by the Rayleigh scattering. Similar comparisons were made for the experiments with outer turbulence of 1% and 18%. Therefore, it was shown during CARS equipment testing that data on the averaged temperatures, obtained by the probe (thermocouple) and optic (CARS) methods for incident flow turbulence of 1-18% coincide.

### Investigation of heat transfer effect on distribution of $\text{OH}$ and $\text{CH}$ radicals in a boundary layer with combustion

The temperatures at hydrogen and ethanol combustion (Boyarshinov & Fedorov, 2004) and concentrations of OH and CH radicals in the boundary layer with ethanol combustion (Boyarshinov *et al.* 2005) were measured by the LIF method.

For measured concentrations of OH radical saturated fluorescence was excited and registered within vibration-rotation band 0-0 of system  $A^2\Sigma^+ - X^2\Pi$ . The laser wavelength was adjusted to spectral peak 3113 Å (Fig.9). This provided  $P_6$  transition from level  $f_6$  to level  $F_5$ . The monochromator with spectral resolution of 3 Å was adjusted to the peak with the wavelength of 3075 Å, formed by an isolated line of  $R_2$  transition from level  $F_5$  to level  $f_4$ . Fluorescence was registered during a short period of time, matched with the maximal intensity of laser radiation pulse. A temperature change within 900-3000 K does not lead to significant redistribution of population at initial level  $f_6$ , therefore, intensity of OH fluorescence, measured by this scheme, depends only on concentration of these radicals.

The density of laser radiation strength in a lens focus ( $f=100$  mm) exceeded the known value of saturation threshold and made up  $3 \cdot 10^7 \text{ W}/(\text{cm}^2 \cdot \text{cm}^{-1})$ . Saturated fluorescence from the center of the focused laser beam with the size of  $0.03 \times 0.1 \times 1.0$  mm, limited by the inlet slit, diameter of beam waist and diaphragm, was sent to the monochromator. For a single measurement temporal resolution of the registration system with consideration of photomultiplier performance was 10 ns, and it was less than laser pulse duration. To determine absolute concentrations, a signal was calibrated in diffuse hydrogen flame, studied previously by Lucht *et al.* (1983) and Lucht *et al.* (1984). For this purpose the conditions of their experiments were reproduced.



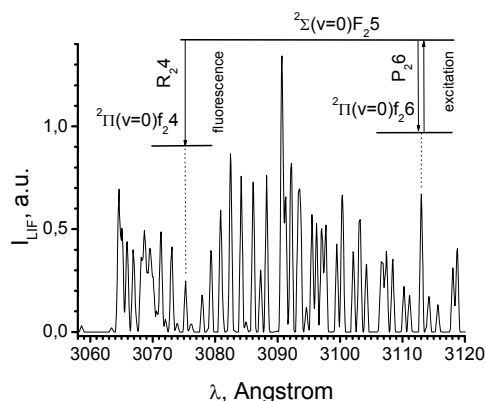


Fig.9. Calculated spectrum ( $T=1749$  K) within band 0-0 and diagram of the LIF process of OH with saturation. Laser excitation at the wavelength of  $P_{26}$  transition. Measurement of fluorescence at the wavelength of  $R_{24}$  transition.

Fluorescence of CH radical was excited within band 0-0 of system  $B^2\Sigma^- - X^2\Pi$  (Boyarshinov *et al.* 2005). The laser wavelength was scanned near peak 3907 Å, formed by lines  $Q_1(8)$  and  $Q_2(8)$ , low-sensitive to temperature. Integral fluorescence within band 0-1 was registered at monochromator adjustment with resolution of 150 Å to wavelength 4350 Å. Relative concentration of CH radicals was measured since there was no LIF signal calibration in this case.

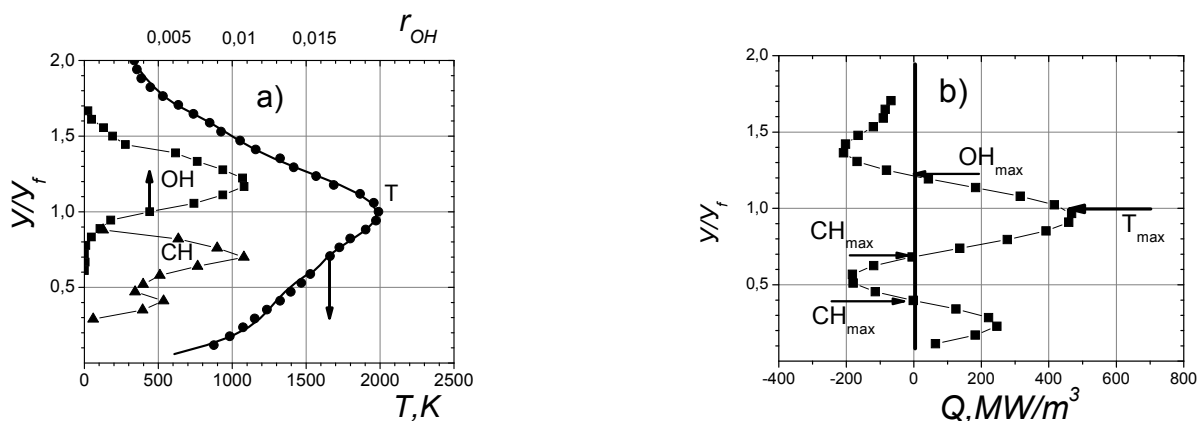


Fig.10. Combustion of ethanol on the surface of a porous sphere with the diameter of 15 mm. A shift of maximal concentrations of  $\square$  and  $\triangle$  radicals relative to the flame front ( $\square$ ); coincidence of their coordinates with the boundaries of heat transfer area (b).

The most important characteristics of combustion (rate of flame propagation, combustion efficiency, etc.) can be determined on the basis of radical distribution, which depends on reaction kinetics, gas-dynamic and thermal characteristics. It was shown in (Volchkov *et al.* 2006) that at ethanol combustion within a boundary layer, the OH and temperature maximums shift relative to each other. This shift does not correspond to the flame front model; it is kept for incident flow turbulence of 1%, 8% and 18%. It is known for diffusion combustion of hydrogen that concentration of  $\square$  radical exceeds the equilibrium values (Lucht *et al.* 1984).

To study the reasons, causing these features of diffusion combustion, the effect of heat transfer on the structure of the zone of chemical transformations was analyzed. Experimental data for three types of

reacting flows were considered. Among them there are the frontal point of a sphere, modeling droplet combustion; the boundary layer behind a stabilizer of 3-mm height (incident flow turbulence of 1%, 8% and 18%), and the jet of hydrogen burning in air. Data for the frontal point of the sphere with 15-mm diameter are shown in the Fig.10. The profiles of OH and  $\text{H}_2\text{O}_2$  radicals, temperature ( $\text{K}$ ) and distributions of heat transfer intensity (b), actually determined by the second derivative for the temperature curve, are compared there. It can be seen that positions of  $\text{H}_2\text{O}_2$  and  $\text{H}_2\text{O}$  maximums coincide with the points, where heat transfer intensity passes zero. The shift of the maximums of temperature and hydroxyl OH profiles and firstly discovered coincidence of OH maximum with the area without heat transfer and chemical transformations is probably a common property of diffusion combustion. It was determined for combustion of a hydrogen jet (Lucht *et al.* 1984) and combustion in a boundary layer behind a flame stabilizer, including the increased up to 18% level of turbulence (Volchkov *et al.* 2006 and Boyarshinov *et al.* 2005).

These results explain the reasons for the areas with superequilibrium concentration of radicals. They should be taken into account by combustion kinetics, including correct interpretation of diffuse flame observations.

### Concerning multicomponent diffusion

Multicomponent diffusion: separation of air components in a boundary layer at foreign gas injection or within the jets of these gases, flowing into air, was studied in (Lukashov & Zhilivostova, 2008). Experiments were carried out with the use of probe methods; they have shown a change in the ratio of oxygen and nitrogen concentrations in the part of the flow, where volumetric concentration of air makes up several percents of the atmospheric concentration and approaches the detection limit. At mathematical modeling of this process (Makarov, 2008) the authors obtain the estimates of this separation value, similar to the experimental results.

Our equipment was used for experimental investigation of the  $\text{O}_2/\text{N}_2$  ratio at jet outflow into air by the optically nonperturbative method. To diagnose the composition, the Raman scattering method on rotational transition of molecules was used. This method allows simultaneous measurements of oxygen and nitrogen concentrations at one point.

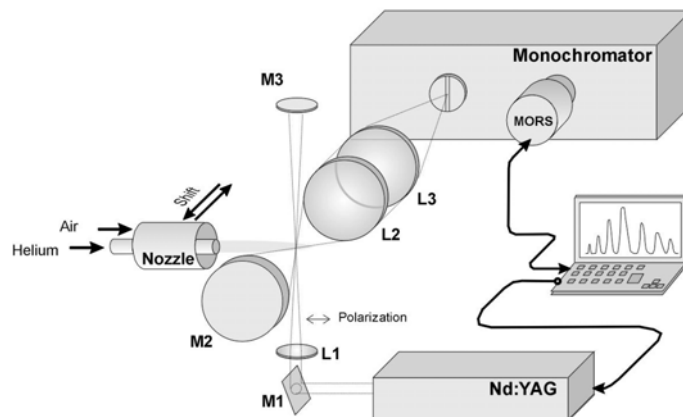


Fig.11. Experimental scheme for jet investigation.

### *Scheme of experiment*

A horizontal jet of helium flew out of a 5-mm nozzle into the co-current air flow (Fig.11). Measurements were carried out over a jet cross-section at a distance of 5 mm from the nozzle. Radiation of second harmonics of the Nd:YAG laser with the wavelength of 532 nm was sent by mirror M1 and focused by lens L1 (F=150 mm) within the measurement region. The laser operated with repetition frequency of 10 Hz and energy of 50 mJ/pulse.

Light scattered from the zone of beam waist was sent to the inlet slit of monochromator DFS-24 by two-lens collecting system L2 and L3. To increase total efficiency of the laser and collecting systems by the factor of 4, reflecting mirrors  $\square 2$  and  $\square 3$  were used. A multichannel optic spectral recorder (MORS) was mounted behind the monochromator instead of the outlet slit. Laser burst and registration of corresponding monopulse spectrum occur synchronously. The series of monopulse spectra were recorded at one flow point. The measurement volume size of  $0.06 \times 0.03 \times 0.07$  mm was determined by the diameter of the focused laser beam (0.06 mm), enlargement of collecting system (3-fold), inlet slot width (0.1 mm) and height of a sensitive element of a detector (0.2 mm). An object was scanned by movement of a nozzle, mounted on a coordinate device. The power of laser radiation was controlled by powermeter IMO-2.

### *Data acquisition and processing*

Intensity and reproducibility of monopulse air spectra were not high; therefore, they were hardly applicable for calculation of instantaneous parameters. To achieve the acceptable accuracy, it was necessary to summarize up to 1000 such spectra and calculate the parameters by the average spectrum for the whole series. At first, the spectral series was measured in air without jet, and the average spectrum was calculated. Then, they were used for calibration by the wavelengths and sensitivity adjustment, required because of inaccurate alignment. Then, the spectral series were measured at some certain points of the flow. The ratio of oxygen/nitrogen concentration was determined by the average spectra:  $R = C(\text{O}_2)/C(\text{N}_2)$ . For this purpose the software for spectrum calculation (Fig.12) with fitting by the mentioned parameter at comparison of the shapes of experimental and calculated spectra, was used.

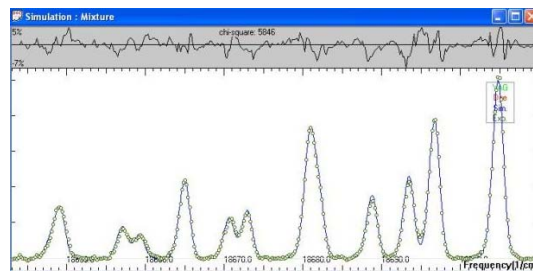


Fig.12. Experimental and calculated spectra of air within the chosen range under the normal conditions with accumulation of 100 pulses.

Air concentration was measured by the total intensity of all lines within the registered spectral range. The profile of air concentration in a helium jet is shown in Fig.13. The corresponding profiles of separation parameter, calculated by formula  $(R-R_0)/R_0$ , where  $R_0=0.268$  is the ratio in air without jet, are shown in Fig.14 (a and b). The profiles are shown depending on the distance from the jet center and volumetric portion of air, respectively. It is obvious that while moving from the periphery to the jet axis, when air concentration decreases from 1 to 0.01, the separation parameter is about zero. Thus, according to data obtained, air separation does not occur with the accuracy of up to the measurement error (random error is 4%).

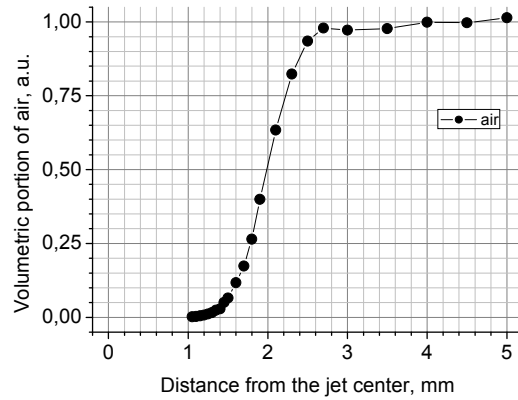


Fig.13. Concentration of air in a helium jet.

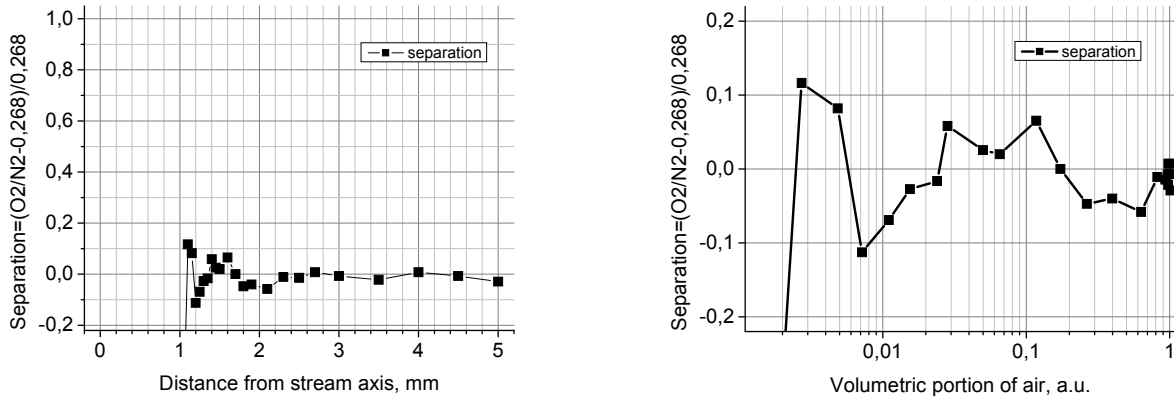


Fig.14. Separation parameter.

## CONCLUSIONS

Therefore, the equipment for simultaneous measurements of temperature and concentration of gases has been developed. It is intended for application of various methods of optic investigations with the use of coherent anti-Stokes light scattering, laser-induced fluorescence, Rayleigh and Raman scattering. This allows obtaining of data on the local temperature, composition and pressure of gases during a burst of laser radiation without introduction of gas-dynamic perturbations into a gas flow. The device is adapted for the use by different aerodynamic installations. It can be used for development of new types of engines in aviation, rocket engineering, car industry, where traditional methods of diagnostics are inapplicable.

## ACKNOWLEDGMENTS

The authors would like to acknowledge the RFBR (project 09-03-00471-a), which supported this work. The construction of the multipurpose CARS-spectrometer was supported by the Foundation for Assistance to Small Innovative Enterprises (projects No. 3886 and No. 2887/14801) and Siberian Branch of the Russian Academy of Sciences (integration project No. 28).

## REFERENCES

- V.I. Kuznetsov (1994), *Teoriya j raschet effekta Ranka (Theory and Calculation of the Ranque Effect)*, Omsk: Omsk Gos. Tekh. Univ.
- B.F. Boyarshinov and S.Yu. Fedorov (1999) “Coherent anti-Stokes Raman scattering technique for investigating parameters of a vortex gas flow”, *Instruments and Experimental Techniques*, **42**(6), 80-84.
- S.Yu. Fedorov (1996) “Alternative phase-matching in CARS”, *Instruments and Experimental Techniques*, **39**(1), 110-114.
- B.F. Boyarshinov and S.Yu. Fedorov (2002) “Measurement of the combustion temperature of a solid propellant by the CARS method”, *Journ. Applied Mech. and Tech. Physics*, **43**(6), 925-929.
- B.F. Boyarshinov and S.Yu. Fedorov (2004), “Measurement of Temperature and Concentration of OH radicals in Combustion of Hydrogen and Ethanol”, *Comb., Explos. and Shock Waves*, **40**(5), 511-515.
- B.F. Boyarshinov, V.I. Titkov and S.Yu. Fedorov (2005), “Distribution of OH and CH Radicals in the Boundary Layer with Ethanol Combustion”, *Combustion, Explosion, and Shock Waves*, **41**(4), 379-385.
- R.P. Lucht, D.W. Sweeney, N.M. Laurendeau et al. (1983), “Laser-saturated fluorescence measurements of OH concentration in flames”, *Combust. Flame*, **50**(3), 189–205.
- R.P. Lucht, D.W. Sweeney, N.M. Laurendeau et al. (1984), “Single-pulse, laser-saturated fluorescence measurements of OH in turbulent nonpremixed flames”, *Opt. Lett.* **9**(3), 90 – 92.
- E.P. Volchkov, V.V. Terekhov, S.Yu. Fedorov, and B.F. Boyarshinov (2006), “Boundary layer with combustion over permeable surface”, pp.63-90 in *Zakony Gorenia (Combustion laws)*, Ed. by Yu.V. Polezhaev, M.: Energomash.
- V.V. Lukashov, S.V. Zhilivostova (2008), “Properties of multicomponent diffusion in laminar boundary layer with foreign injection”, *Thermophysics and Aeromechanics* **15**(3), 505-511.
- M.S. Makarov (2009), “Numerical method for multicomponent diffusion with a posteriori evaluation of calculation accuracy on the basis of mass balance”, *Int. Journal of Heat and Mass Transfer* **52**(7-8), 1769-1773.